Stefan Pollnow*, Areg Noshadi, Michael Kircher, Gisela Guthausen, Thomas Oerther and Olaf Dössel

3D reconstruction of ablation lesions from in-vitro preparations using MRI

Abstract: Radiofrequency ablation is the gold standard for treating cardiac arrhythmias. However, the success rate of this procedure depends on numerous parameters. Wet lab experiments provide the opportunity to investigate cardiac electrophysiology under reproducible conditions. To evaluate the electrophysiological changes of ablated myocardium in these studies it is necessary to consider the three-dimensional (3D) geometry of the lesions. For this purpose, we investigated the usage of different magnetic resonance imaging (MRI) sequences as well as an image processing procedure to analyze *in-vitro* preparations. To differentiate signal intensities between nonablated and ablated tissue we evaluated FISP (fast imaging with steady-state precession; delivering dominantly T_1-weighted images) and RARE (rapid acquisition with relaxation enhancement; delivering dominantly T_2-weighted images). After image processing, the ablated tissue was segmented in each image slice forming a 3D volume. The geometry of the lesion was modeled by the boundary of this volume. It was generally feasible to distinguish between healthy myocardium and ablated tissue as well as to determine lesion transmurality. The analysis of the reconstructed lesion geometries from FISP and RARE MRI showed a high agreement, however T_2-weighted sequences showed larger lesion volumes as well as higher variations in segmentation compared to T_1-mapping. FISP with higher quality may be used to reconstruct the 3D geometry of the ablation lesions.

Keywords: MRI, ablation lesions, *in-vitro*, rat myocardium, wet lab experiments.

1 Introduction

About one quarter of all people aged 40 or older will suffer from atrial fibrillation (AF) in their coming life. AF leads to an increased risk of stroke and heart failure [1]. Radiofrequency ablation (RF-ablation) is the gold standard to treat cardiac arrhythmias. However, the success rate of this therapy is relativley moderate [2]. A corner stone of RF-ablation is the formation of transmural lesions as well as gapless lesion lines [3]. Wet lab experiments allow to investigate cardiac electrophysiology as well as pathophysiology under well-defined conditions with high spatio-temporal resolution [4]. Subsequent histological investigations are required to determine the microscopic structure. Several groups also reconstructed the three-dimensional (3D) structure of the tissue using either magnetic resonance imaging (MRI) measurements or a combination of MRI and histology [5–7]. At the Institute of Biomedical Engineering (IBT) we established an *in-vitro* setup to investigate cardiac electrophysiology of rat myocardium with acute ablation lesions using fluorescence-optical as well as electrical techniques. In order to investigate changes of electrical activity of myocardium surrounding the lesion it is required to analyze the 3D geometry of the lesions. In this study, we focused on two different MRI sequences in order to evaluate 3D geometry as well as transmurality of the ablation lesions.

2 Methods

2.1 In-vitro preparations

During our *in-vitro* experiments, the myocardium is positioned in a tissue bath with heated Krebs-Henseleit solution, which allows the nutrition and oxygenation of the preparation. Fluorescence-optical mapping, using a voltage-sensitive dye (di-4-ANEPPS), and electrical recordings with a multi-electrode array are performed from either the bottom or the top side of the tissue bath. We are using the electrosurgical unit MD1 (Micromed, Wurmlingen, Germany) for performing an *in-vitro* RF-ablation. Hereby, the RF-ablation electrode (diameter of 0.3 mm) is placed perpendicular onto the surface of

_____

*Corresponding author: Stefan Pollnow:** Institute of Biomedical Engineering, Karlsruhe Institute of Technology (KIT), Kaiserstr. 12, 76128 Karlsruhe, Germany, e-mail: publications@ibt.kit.edu
Areg Noshadi, Michael Kircher, Olaf Dössel: Institute of Biomedical Engineering, Karlsruhe Institute of Technology (KIT), Kaiserstr. 12, 76128 Karlsruhe, Germany
Gisela Guthausen: Institute of Mechanical Process Engineering and Mechanics (MVM) and Engler-Bunte-Institute, Chair of Water Chemistry and Water Technology, Karlsruhe Institute of Technology (KIT), Adenauerring 20b, 76131 Karlsruhe, Germany
Thomas Oerther: NMR Microscopy Applications, Bruker BioSpin GmbH, Silberstreifen 4, 76287 Rheinstetten, Germany

the tissue to create varying ablation lesions. To establish an appropriate MRI sequence, the *in-vitro* RF-ablation procedure was at first performed with freshly, excised rat myocardium gained post mortem instead of living cardiac tissue. The right ventricle, having an approximate thickness of 1 mm, was excised from the heart and fixed on a silicone holder. Either one or multiple point-shaped ablation lesions were created with an ablation power of 2 W over a time duration of approximately 3 s. After the RF-ablation, the preparation was fixated for 24 hours in paraformaldehyde. Subsequently, the preparation was washed several times with water and stored in phosphate buffered saline (PBS). For the MRI measurements, we used three pieces of ventricles having one or two ablation lesions. Moreover, a silicone holder with a diameter of approximately 9.8 mm was constructed for a stable positioning of the preparations in a glass tube having a diameter of 10 mm. This tube was inserted into the MRI device.

2.2 MRI measurements

The MRI measurements were performed with a 4.7 T nuclear magnetic resonance (NMR) device (Bruker Avance 200) at the Institute for Mechanical Process Engineering and Mechanics (MVM, KIT, Karlsruhe). The system was equipped with microimaging, wide-bore (MIC-WB) probes and Paravision software for image acquisition. Measurement temperature was 20°C. In order to differentiate ablated tissue from nonablated tissue we investigated the applicability of the following imaging sequences: T_1- or T_2-weighted imaging, diffusion imaging, inversion recovery sequence and T_1-weighted imaging with gadolinium-based contrast agents according to Hansen *et al.* [8]. However, only fast imaging with steady-state precession (FISP) and rapid acquisition with relaxation enhancement (RARE) sequences resulted in sufficient image contrast. FISP delivered dominantly T_1-weighted images, RARE delivered dominantly T_2-weighted images. The acquired FISP and RARE images had a digital resolution of 256×128 pixels with a field of view (FOV) of 10 mm×5 mm or 9 mm×4.5 mm. The data sets contained up to 20 slices with slice distances of 0.3-0.35 mm and slice thickness of 0.2 mm. Figure 1 shows one slice of the raw data recorded by FISP sequence as well as after image processing.

2.3 Image processing

The raw data was stored in a proprietary format by Bruker which had to be imported into MATLAB 9.1 (The MathWorks
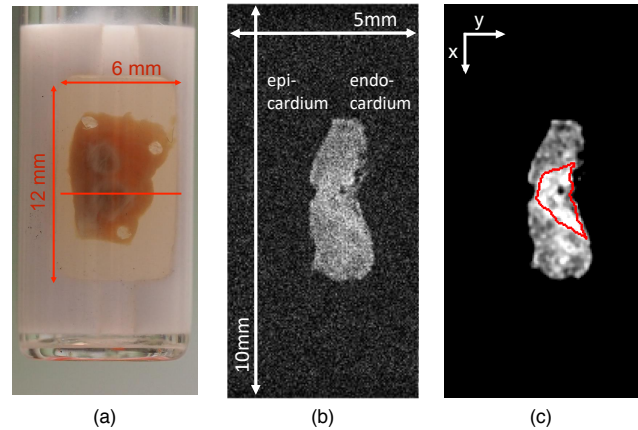
Figure 1: Ventricle sample with two ablation lesions (Sample 1) (a). The raw MRI slice (b, FISP image) shows a cross-section through the red line in (a). After image processing ablated tissue was segmented ten times in this cross-section. The red line represents the perimeter of the region included in all segmentations (c).

Inc., Natick, Massachusetts, USA). The raw images were noisy as well as partially corrupted by fold-over artifacts due to the samples geometry. Firstly, a median filter having a filter kernel of 3×3 pixel was applied to remove impulse noise and outliers. Afterwards, a Gaussian filter was used to reduce white noise. Due to varying noise level in different data sets, σ was set manually for all raw images of one imaging sequence (between 0.5 and 1). Subsequently, a method was implemented, which improved the image contrast by automatically analyzing the image histogram. In general, the histograms showed two distinct peaks after filtering. Pixels comprising the sample were represented by a certain range of gray values located around the smaller peak. The latter one described the background pixels. The gray value corresponding to the minimum in between the two peaks was defined as the lower limit, while the upper limit was defined as the gray value, where the frequency had dropped to 10 %. Generally established segmentation methods, e.g. region growing or active contour models, could not determine lesion edges due to several reasons, e.g. either fold-over artifacts or no clear differentiation of tissue contrast. Regarding these challenges as well as the limited number of slices in the recorded data sets (maximum 20 slices) manual segmentation had to be applied. Slice by slice, the region of interest (ROI) was manually selected and a binary segmentation mask was created. In order to reconstruct the 3D geometry, a bounding volume had to be formed from the segmented areas of the slices. Therefore, the boundary points of the binary segmentation masks were interpreted as point coordinates located in a plane parallel to the *xy*-plane (resolution: 35-39 μm) and slice numbers increased in *z*-direction (resolution: 300-350 μm). Using the *alphaShape* function ($\alpha = 15$)

of MATLAB 9.1, a polyhedron hull was created for the given lesion perimeter points.
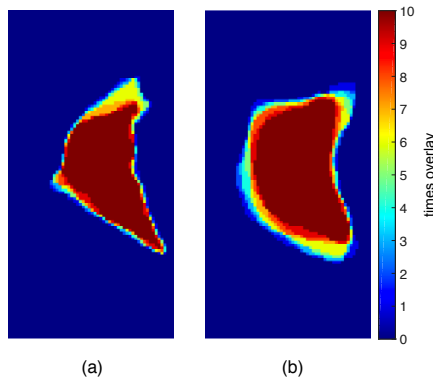
Figure 2: Overlay of FISP (a) and RARE (b) segmented areas in slice 6 from the ten times segmented data sets of Sample 2. The ten times segmented area of the FISP slice (presented in dark red) is plotted in Figure 1(c).
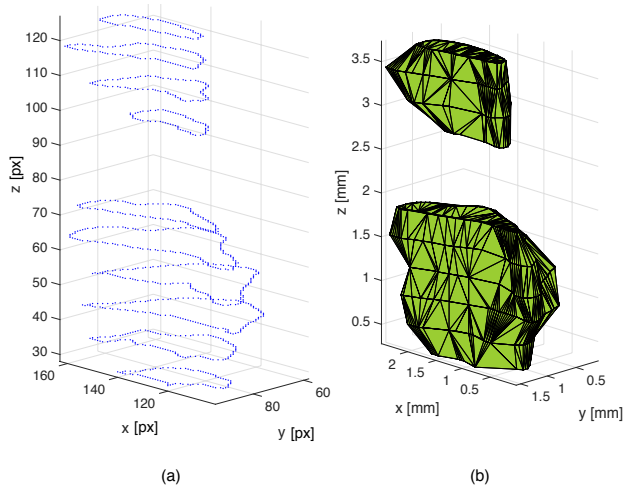
Figure 3: Lesion perimeter points of the segmented areas in z-direction (a) and 3D lesion model (b) of the sample shown in Figure 1(a). The endocardial surface is at the left side.

3 Results

One FISP and one RARE data set from one preparation (here called Sample 2) with comparatively good quality was segmented ten times. The resulting segmentation masks and 3D lesion models were used to determine the robustness of the manual segmentation and deviation in lesion volumes (see Figure 2). Additionally, the mean volumes of the two lesions in Sample 2 were determined (see Table 1). The RARE data set delivered higher volumes for both lesions. The difference of the mean FISP and RARE volume was significantly

Table 1: Mean lesion volumes and standard deviations from the ten times segmented data sets of Sample 2

	Mean lesion volume	
	FISP	**RARE**
$V_{\mu,1}$ [mm^3]	1.945	1.989
$V_{\mu,2}$ [mm^3]	0.569	0.771
	Standard deviation of lesion volume	
	FISP	**RARE**
σ_1 [mm^3]	0.086	0.190
σ_2 [mm^3]	0.041	0.051

higher for the smaller lesion. Standard deviations of the RARE volumes were also higher. Remarkable is the fact that the standard deviation of the larger lesion σ_1 was more than double the deviation of the FISP lesion. It was also examined if transmurality of the lesions could be determined from the segmentation results of Sample 2. Therefore, we analyzed the segmented slices with the largest lesion crosssection area of the sample. By looking at the regions that were segmented ten times, it can be assumed that these regions were definitely lesion tissue. However, these regions did not reach all the way through the myocardium. Furthermore, a second preparation (here called Sample 1) was measured twice with the same RARE sequence, but with a slice offset of 0.1 mm. The two data sets were merged. The lesion volumes were modeled in the same way as the other data sets of Sample 2, but this time the resolution in z-direction was improved by a factor of 2 (no equidistant distances). The segmented lesion areas had noticeable fluctuations causing an uneven lesion surface.

4 Discussion

In this study, various MRI sequences were studied in order to differentiate ablated and nonablated tissue as well as to reconstruct 3D geometry of the ablation lesions without using gadolinium-based contrast agents. Finally, FISP (dominantly T_1-weighted images) as well as RARE imaging sequences (dominantly T_2-weighted images) delivered an appropriate image quality to distinguish ablated and nonablated tissue. The acquired images are comparable to the *ex-vivo* gadolinium enhanced MRI studies from Hansen *et al.* [8]. Other imaging techniques did not deliver evaluable results due to insufficient data quality. We also performed an experiment with contrast agents according to the experimental protocol from the previous study [8], but image quality as well as contrast did not improve significantly compared to our FISP and RARE MRI. Subsequent image processing, including noise reduction and

an automatic contrast enhancement, changed the visibility of the lesion significantly. It was feasible to reconstruct the 3D geometry of the ablation lesion with both imaging sequences in our study. Manual segmentation was the most suitable and robust solution for identifying the lesion border in each image due to high noise, low contrast as well as artifacts. However, the variation in the manual slice segmentation was high for both FISP and RARE images. The raw RARE images had better lesion visibility while the raw FISP images were strongly affected by noise. After image processing, lesion boundaries were better defined in the FISP images. While the mean FISP and RARE lesion volumes did not substantially differ, the deviation of the larger lesion volume $\sigma 1$ reconstructed from RARE data was more than twice the deviation of the FISP volume (see Table 1). One possible explanation could be that lesion tissue was detected with higher uncertainty in RARE slices while the lesion was detected more reliable in the FISP slices. To conclude, the volume and the geometry of the lesions were determined more precisely with FISP MRI than RARE MRI. Investigating lesion transmurality based on one-time segmented slices were vulnerable because of the previously explained inaccuracy of the segmentation. These inaccuracies were compensated by considering the lesion regions that were segmented ten times. Although Figure 1(c) suggests that the lesion was not transmural in this sample, further histological examinations are necessary to ensure the presence of either transmural or nontransmural lesions determined by *ex-vivo* MRI and this multiple segmentation approach. Using multiple measurements with different offsets of 0.1 mm increment to increase the slice numbers and hence to improve the resolution is possible. The measurements with the offset RARE data set resulted in a lesion model with fluctuating lesion areas. This effect was caused by the inaccuracy of multiple manual segmentation leading to higher variation of the lesion extensions. Furthermore, it has to be mentioned that the distance of the offset slices was not ideal. The RARE measurements delivered slices with a slice thickness of 0.214 mm and a slice gap of 0.1 mm. In future studies, the method of using offset measurements to increase the resolution may succeed if the segmentation of the slices is more accurate, the slice number is increased, and the slices in the combined data set are placed equidistantly. Moreover, it may be possible to obtain better results with new higher quality data performing FISP imaging without gadolinium based-contrast agents as well as using our developed algorithms. Thus, the lesion models could be more precise and have a higher informative value regarding shape and transmurality. Additionally, these results should also be compared to histology in order to confirm the results of the *ex-vivo* MRI.

References

[1] Stewart, Hart CL, Hole DJ, McMurray JJ. A population-based study of the long-term risks associated with atrial fibrillation: 20-year follow-up of the Renfrew/Paisley study. Am J Med 2002; 113(5): 359-364.

[2] Shurrab M, Biase LD, Briceno DF, et al. Impact of Contact Force Technology on Atrial Fibrillation Ablation: A Meta-Analysis. J Am Heart Assoc 2015; 4(9): e002476.

[3] Calkins H, Kuck KH, Cappato R, et al. 2012 hrs/ehra/ecas expert consensus statement on catheter and surgical ablation of atrial fibrillation: Recommendations for patient selection, procedural techniques, patient management and follow-up, definitions, endpoints, and research trial design. J Interv Card Electrophysiol 2012; 33(2): 171-257.

[4] Efimov IR, Nikolski VP, and Salama G. Optical imaging of the heart. Circ Res 2004; 95(1): 21-33.

[5] Burton RAB, Plank G, Schneider JE, et al. Three-dimensional models of individual cardiac histoanatomy: tools and challenges. Ann N Y Acad Sci 2006; 1080: 301-19.

[6] Schelbert EB, Hsu LY, Anderson SA, et al. Late gadolinium-enhancement cardiac magnetic resonance identifies postinfarction myocardial fibrosis and the border zone at the near cellular level in ex vivo rat heart. Circ Cardiovasc Imaging 2010; 3(6): 743-52.

[7] Bishop MJ, Plank G, Burton RA, et al. Development of an anatomically detailed MRI-derived rabbit ventricular model and assessment of its impact on simulations of electrophysiological function. Am J Physiol Heart Circ Physiol 2010; 298(2): H699-718.

[8] Hansen BJ, et al. Atrial fibrillation driven by micro-anatomic intramural re-entry revealed by simultaneous sub-epicardial and sub-endocardial optical mapping in explanted human hearts. Eur Heart J 2015; 36(35): 2390-401.